

掲載した論文（発表題目）	発表者氏名	発表した場所 (学会誌・雑誌等 名)	発表した時期	国内・外の別
Therapeutic potential of midkine in cardiovascular disease	Kadomatsu K, Bencsik P, Görbe A, Csonka C, Sakamoto K, Kishida S, Ferdinandy P	Br J Pharmacol. 171(4):936-44	2014	国外
Aggressive transformation of anaplastic large cell lymphoma with increased number of ALK-translocated chromosomes.	Hoshino A, Nomura K, Hamashima T, Isobe T, Seki M, Hiwatari M, Yoshida K, Shiraishi Y, Chiba K, Tanaka H, Miyano S, Ogawa S, Takita J, Kanegane H.	Int J Hematol. 101:198-202	2015	国外
Early use of allogeneic hematopoietic stem cell transplantation for infants with MLL gene-rearrangement-positive acute lymphoblastic leukemia.	Koh K, Tomizawa D, Moriya Saito A, Watanabe T, Miyamura T, Hirayama M, Takahashi Y, Ogawa A, Kato K, Sugita K, Sato T, Deguchi T, Hayashi Y, Takita J, Takeshita Y, Tsurusawa M, Horibe K, Mizutani S, Ishii E.	Leukemia. 29:290-6	2015	国外
Allogeneic haematopoietic stem cell transplantation for infant acute lymphoblastic leukaemia with KMT2A (MLL) rearrangements: a retrospective study from the paediatric acute lymphoblastic leukaemia working group of the Japan Society for Haematopoietic Cell Transplantation.	Kato M, Hasegawa D, Koh K, Kato K, Takita J, Inagaki J, Yabe H, Goto H, Adachi S, Hayakawa A, Takeshita Y, Sawada A, Atsuta Y, Kato K.	Br J Haematol. 168:564-70.	2015	国外

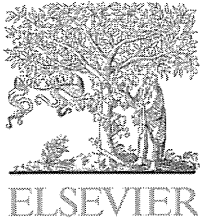
掲載した論文（発表題目）	発表者氏名	発表した場所 (学会誌・雑誌等 名)	発表した時期	国内・外の別
Identification of a homozygous JAK3 V674A mutation caused by acquired uniparental disomy in a relapsed early T-cell precursor ALL patient.	Kawashima-Goto S, Imamura T, Seki M, Kato M, Yoshida K, Sugimoto A, Kaneda D, Fujiki A, Miyachi M, Nakatani T, Osone S, Ishida H, Taki T, Takita J, Shiraishi Y, Chiba K, Tanaka H, Miyano S, Ogawa S, Hosoi H.	Int J Hematol.	2014 Nov 28. [Epub ahead of print]	国外
Cyclic fluctuation of blood pressure in neonatal neuroblastoma.	Fujishiro J, Sugiyama M, Ishimaru T, Uotani C, Tsuchida S, Takahashi N, Shiozawa R, Takita J, Iwanaka T.	Pediatr Int. 56:934-7	2014	国外
Systemic lupus erythematosus complicated with liver cirrhosis in a patient with Papillon-Lèfevre syndrome.	Yasudo H, Ando T, Takeuchi M, Nakano H, Itonaga T, Takehara H, Isojima T, Miura K, Harita Y, Takita J, Oka A.	Lupus. 23:1523-7	2014	国外
Prognostic significance of leukopenia in childhood acute lymphoblastic leukemia.	Shiozawa Y, Takita J, Kato M, Sotomatsu M, Koh K, Ida K, Hayashi Y.	Oncol Lett. 7:1169-74	2014	国外
Relapsed Acute Lymphoblastic Leukemia with Unusual Multiple Bone Invasions: A case report.	Hangai M, Watanabe K, Shiozawa R, Hiwatari M, Ida K, Takita J.	Oncol Lett. 7:991-3	2014	国外

掲載した論文（発表題目）	発表者氏名	発表した場所 (学会誌・雑誌等 名)	発表した時期	国内・外の別
Flotillin-1 regulates oncogenic signaling in neuroblastoma cells by regulating ALK membrane association.	Tomiyama A, Uekita T, Kamata R, Sasaki K, Takita J, Ohira M, Nakagawara A, Kitanaka C, Mori K, Yamaguchi H, Sakai R.	Cancer Res. 15;74:3790-801	2014	国外
Biallelic DICER1 mutations in sporadic pleuropulmonary blastoma.	Seki M, Yoshida K, Shiraishi Y, Shimamura T, Sato Y, Nishimura R, Okuno Y, Chiba K, Tanaka H, Kato K, Kato M, Hanada R, Nomura Y, Park MJ, Ishida T, Oka A, Igarashi T, Miyano S, Hayashi Y, Ogawa S, Takita J.	Cancer Res. 74:2742-9	2014	国外
Genome-wide approach to identify second gene targets for malignant rhabdoid tumors using high-density oligonucleotide microarrays.	Takita J, Chen Y, Kato M, Ohki K, Sato Y, Ohta S, Sugita K, Nishimura R, Hoshino N, Seki M, Sanada M, Oka A, Hayashi Y, Ogaw S.	Cancer Sci. 105:258-64	2014	国外
Japanese Dent disease has a wider clinical spectrum than Dent disease in Europe/USA: genetic and clinical studies of 86 unrelated patients with low-molecular-weight proteinuria.	Sekine T, Komoda F, Miura K, Takita J, Shimadzu M, Matsuyama T, Ashida A, Igarashi T.	Nephrol Dial Transplant. 29:376-84.	2014	国外
The effect of the order of total body irradiation and chemotherapy on graft-versus-host disease.	Kato M, Shiozawa R, Koh K, Nagatoshi Y, Takita J, Ida K, Kikuchi A, Hanada R.	J Pediatr Hematol Oncol. 36:e9-12	2014	国外

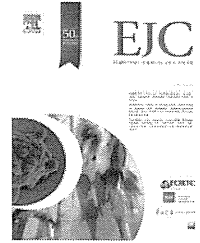
掲載した論文（発表題目）	発表者氏名	発表した場所 (学会誌・雑誌等 名)	発表した時期	国内・外の別
Ectopic Neuroblastoma in Monozygotic Twins With Different Ages of Onset: Possible Twin-to-Twin Metastasis In Utero With Distinct Genetic Alterations After Birth.	Taketani T, Takita J, Ueyama J, Kanai R, Kumori K, Maruyama R, Hayashi K, Ogawa S, Fukuda S, Yamaguchi S.	J Pediatr Hematol Oncol. 36:166-8	2014	国外
小児の臨床検査 小児の遺伝子・染色体検査(解説)	滝田 順子	検査と技術 (0301-2611)43巻1 号 Page58-62	2015	国内
【ビジュアル小児外科疾患のフォローアップ・プログラム-手術直後から遠隔期の問題点まで】 神経芽腫(解説/特集)	滝田 順子	小児外科 (0385- 6313)46巻11号 Page1159-63	2014	国内
高用量シクロフォスファミドによるHLA一致同胞間骨髓幹細胞移植後に致死的心毒性をきたした一例(原著論文/症例報告)	渡邊 健太郎, 加藤 元博, 田中 淳, 中 井 まりえ, 関 正 史, 林 泰佑, 塩澤 亮輔, 樋渡 光輝, 吉田 健一, 小川 誠司, 松坂 恵介, 深山 正久, 滝田 順子, 岡 明.	日本造血細胞移植 学会雑誌 3巻4号 Page120-3	2014	国内
次世代シーケンサーによる小児血液、腫瘍疾患における研究の進展 小児固形腫瘍における治療標的の探索(解説)	滝田 順子	日本小児血液・がん 学会雑誌 (2187-011X)51巻3 号 Page278-84	2014	国内
【小児の治療指針】 血液・腫瘍 悪性リンパ腫(解説/特集).	滝田 順子	小児科診療 (0386-9806)77巻 増刊 Page486-8	2014	国内
【急性リンパ性白血病(ALL)】 小児ALLの予後因子と治療(解説/特集)	滝田 順子	血液内科 (2185- 582X)68巻2号 Page203-9	2014	国内
急性リンパ性白血病に対するゲノム解析の成果	滝田 順子	血液内科. 69:713-9	2014	国内
急性リンパ性白血病(ALL).	滝田 順子	血液フロンティア 24:55-63	2014	国内

掲載した論文（発表題目）	発表者氏名	発表した場所 （学会誌・雑誌等 名）	発表した時期	国内・外の別
神経芽腫の次世代シーケンサーによる解析.	滝田 順子	小児外科47:145-9	2015	国内
TSPAN12 is a critical factor for cancer-fibroblast cell contact-mediated cancer invasion	Ryo otomo, Chihiro Otsubo, Yuko Matsushima-Hibiya, Makoto Miyazaki, Fumio Tashiro, Hitoshi Ichikawa, Takashi Kohno, Takahiro Ohiya, Uun Yokota, Hitoshi Nakagawa, Yoichi Taya, and Masato Enari	Proseeding of the National Academy of Sciences of the United States of America	2014 Dec 30:111(52):18691-18696	国外
Druggable Oncogene Fusions in Invasive Mucinous Lung Adenocarcinoma	Takashi Nakaoku, Koji Tsuta, Hitoshi Ichikawa, Kouya Shiraishi, Hiromi Sakamoto, Masato Enari, Koh Furuta, Yoko Shimada, Hideaki Ogiwara, Shunichi Watanabe, Hiroshi Nokihara, Kazuki Yasuda, Masaki Hiramoto, Takao Nammo, Aaron J.Schetter, Hirokazu Okayama, Curtis C. Harris, Young Hak Kim, Michiaki Mishima, Jun Yokota, Teruhiko Yoshida and Takashi Kohno	Clinical Cancer Reserch	2014 Jun 15;20(12):3087-3093	国外

掲載した論文（発表題目）	発表者氏名	発表した場所 (学会誌・雑誌等 名)	発表した時期	国内・外の別
TSPAN2 is Involved in cell Invasion and Motility during Lung Cancer Progression	Chihiro Otsubo, Ryo Otomo, Makoto Miyazaki, Yuko Matsushima-Hibiya, Takashi Kohno, Reika Iwakawa, Fumitaka Takeshita, Hirokazu Okayama, Hitoshi Ichikawa, Hideyuki Saya, Tohru Kiyono, Takahiro Ochiya, Fumio Tashiro, Hitoshi Nakagama, Jun Yokota, and Masato Enari	Cell Reports	2014 Apr 24:7(2):527-538	国外
Flotillin-1 regulates oncogenic signaling in neuroblastoma cells by regulating ALK membrane association.	Tomiyama A, Uekita T, Kamata R, Sasaki K, Takita J, Ohira M, Nakagawara A, Kitanaka C, Mori K, Yamaguchi H, Sakai R.	Cancer Res. 74(14) :3790-801, 2014	2014/5/15	国外
Revised risk estimation and treatment stratification of low- and intermediate-risk neuroblastoma patients by integrating clinical and molecular prognostic markers.	Oberthuer A, Juraeva D, Hero B, Volland R, Sterz C, Schmidt R, Faldum A, Kahlert Y, Engesser A, Asgharzadeh S, Seeger R, Ohira M, Nakagawara A, Scaruffi P, Tonini GP, Janoueix-Lerosey I, Delattre O, Schleiermacher G, Vandesompele J, Speleman F, Noguera R, Piqueras M, Bénard J, Valent A, Avigad S, Yaniv I, Grundy RG, Orthmann M, Shao C, Schwab M, Eils R, Simon T, Theissen J, Berthold F, Westermann F, Brors B, Fischer M.	Clin. Cancer Res., in press	2014/9/17	国外

Available at www.sciencedirect.com

ScienceDirect

journal homepage: www.ejcancer.com

Novel 1p tumour suppressor Dnmt1-associated protein 1 regulates MYCN/ataxia telangiectasia mutated/p53 pathway

Yohko Yamaguchi^a, Hisanori Takenobu^a, Miki Ohira^b, Atsuko Nakazawa^c, Sayaka Yoshida^a, Nobuhiro Akita^a, Osamu Shimozato^a, Atsushi Iwama^d, Akira Nakagawara^e, Takehiko Kamijo^{a,*}

^a Division of Biochemistry and Molecular Carcinogenesis, Chiba Cancer Center Research Institute, Japan

^b Laboratory of Cancer Genomics, Chiba Cancer Center Research Institute, Japan

^c Department of Pathology, National Center for Child Health and Development, Japan

^d Department of Cellular and Molecular Medicine, Graduate School of Medicine, Chiba University, Chiba, Japan

^e Division of Biochemistry and Innovative Cancer Therapeutics, Chiba Cancer Center Research Institute, Japan

KEYWORDS

DMAP1
ATM
p53
Neuroblastoma
MYCN

Abstract Neuroblastoma (NB) is a paediatric solid tumour which originates from sympathetic nervous tissues. Deletions in chromosome 1p are frequently found in unfavourable NBs and are correlated with v-myc avian myelocytomatosis viral oncogene neuroblastoma derived homolog (*MYCN*) amplification; however, it remains to be elucidated how the 1p loss contributes to MYCN-related oncogenic processes in NB. In this study, we identified the role of Dnmt1-associated protein 1 (DMAP1), coded on chromosome 1p34, in the processes. We studied the expression and function of DMAP1 in NB and found that low-level expression of DMAP1 related to poor prognosis, unfavourable histology and 1p Loss of heterozygosity (LOH) of primary NB samples. Intriguingly, DMAP1 induced ataxia telangiectasia mutated (ATM) phosphorylation and focus formation in the presence of a DNA damage reagent, doxorubicin. By DMAP1 expression in NB and fibroblasts, p53 was activated in an ATM-dependent manner and p53-downstream pro-apoptotic Bcl-2 family molecules were induced at the mRNA level, resulting in p53-induced apoptotic death. *BAX* and *p21^{Cip1/Waf1}* promoter activity dependent on p53 was clearly up-regulated by DMAP1. Further, MYCN transduction in *MYCN* single-copy NB cells accelerated doxorubicin (Doxo)-induced apoptotic cell death; MYCN is implicated in DMAP1 protein stabilisation and ATM phosphorylation in these situations. DMAP1 knockdown attenuated MYCN-dependent ATM phosphorylation and NB cell apoptosis. Together, DMAP1

* Corresponding author: Address: Division of Biochemistry and Molecular Carcinogenesis, Chiba Cancer Center Research Institute, 666-2 Nitona, Chuo-ku, Chiba 260-8717, Japan. Tel.: +81 43 264 5431; fax: +81 43 265 4459.

E-mail address: tkamijo@chiba-cc.jp (T. Kamijo).

<http://dx.doi.org/10.1016/j.ejca.2014.01.023>

0959-8049/© 2014 Elsevier Ltd All rights reserved.

Please cite this article in press as: Yamaguchi Y. et al., Novel 1p tumour suppressor Dnmt1-associated protein 1 regulates MYCN/ataxia telangiectasia mutated/p53 pathway, *Eur J Cancer* (2014), <http://dx.doi.org/10.1016/j.ejca.2014.01.023>

appears to be a new candidate for a 1p tumour suppressor and its reduction contributes to NB tumourigenesis via inhibition of MYCN-related ATM/p53 pathway activation.

© 2014 Elsevier Ltd All rights reserved.

1. Introduction

Genetic and molecular analyses have indicated various types of deletions of the short arm of chromosome 1 (1p) in a broad range of human malignant tumours, including neuroblastoma (NB) and others [1–5]. It has been suggested that this genomic region harbours several tumour suppressor genes and that additive effects of loss of those tumour suppressors on tumourigenesis exist in several ‘1p loss malignant tumours’.

NB is the second most common paediatric solid malignant tumour derived from sympathetic nervous tissues. Extensive cytogenetic and molecular genetic studies have identified that genetic abnormalities, such as loss of the short arm of 1p, 11q and 14q; amplification of *MYCN*; and allelic gain of 11p and 17q, are frequently observed [1]. Deletion of the 1p region is highly correlated with both *MYCN* amplification and an adverse patient outcome, indicating the presence of several tumour suppressor genes (TSGs) within this region [6]. NB tumours with *MYCN* in a single copy had preferentially lost the 1p36 allele and these tumours also had a very distal commonly deleted region; in contrast, all *MYCN*-amplified NBs had larger 1p deletions, extending from the telomere to 1p31 [7]. The extent of deletion or LOH was identified in 184 primary NBs; in 80%, the 1p deletion extended from the telomere to 1p31 [8]. Given the tendency of large, hemizygous 1p deletions in *MYCN*-amplified NBs, alternative hypotheses for tumour suppression are: (1) an additional, *MYCN*-associated TSG in the 1p region; (2) suppression of TSG expression from a hemizygous allele due to epigenetic modifications except for imprinting, e.g. miRNAs and non-coding RNAs; (3) haplo-insufficiency-based suppression accounting for the rarity of 1p homozygous deletions [9].

Dnmt1-associated protein 1 (DMAP1) was originally identified as a molecule interacting with DNMT1 and was demonstrated to co-localise with PCNA and DNMT1 at DNA replication foci during the S phase [10]. Previously, we reported that Dmap1 participates in DNA repair and transformation of mouse embryonic fibroblasts (MEFs). Dmap1 was recruited to the damaged sites, formed complexes with γ -H2AX and directly interacted with Proliferating Cell Nuclear Antigen (Pcna); inhibition of this binding impaired the accumulation of the Pcna-Caf-1 complex at damaged sites and resulted in DNA breaks [11]. In addition, Penicud and Behrens reported that DMAP1 promotes ataxia telangiectasia mutated (ATM) recruitment and focus formation at damaged sites. These results suggest that DMAP1 is involved in the DNA damage response (DDR) [12]. Interestingly,

DMAP1 gene is coded in 1p34 and the region that is frequently deleted in NB tumours with 1p LOH [8,9]. These results prompted us to study the expression level of DMAP1 in neuroblastoma samples and its functional role in tumourigenesis.

In the present report, for the first time, we found that DMAP1 is a novel 1p tumour suppressor and DMAP1 has an indispensable role in MYCN-related ATM/p53 pathway activation. Downregulation of DMAP1 seems to be a result of MYCN-induced stress and an important mechanism for NB tumourigenesis.

2. Materials and methods

2.1. Cell culture

Human NB cell lines were obtained from official cell banks (RIKEN Bioresource Cell Bank, Tohoku University Cell Resource Center, and the American Type Culture Collection) and were cultured in RPMI1640 or Dulbecco’s modified Eagle’s medium (Wako, Osaka, Japan) supplemented with 10% heat-inactivated foetal bovine serum (Invitrogen, Carlsbad, CA, United States of America (USA)) and 50 μ g/ml penicillin/streptomycin (Sigma–Aldrich, St. Louis, MO, USA) in an incubator with humidified air at 37 °C with 5% CO₂. ATM kinase inhibitor, KU-55933 (Santa Cruz Biotechnology, Santa Cruz, CA, USA) was dissolved in DMSO to make stock solutions of 20 mM.

2.2. Lentiviral production and infection for over-expression and knockdown of genes

For the over-expression of mouse Dmap1 and human DMAP1, cDNAs were subcloned into lentiviral vector pHR-SIN-CSGW [13]. For shRNA-based knockdown experiments, pLKO.1 puromycin-based lentiviral vectors containing five sequence-verified shRNAs targeting human DMAP1 (RefSeq NM_019100.4, NM_001034024.1, NM_001034023.1) were obtained from the MISSION TRC-Hs 1.0 Human, shRNA library (Sigma–Aldrich). We checked DMAP1 knockdown by five lentivirus-produced shRNAs (clones: TRCN0000021744–21748) and used at least two shRNAs for experiments. Lentiviral production, infection and confirmation of infection efficiency were performed as described previously [13].

2.3. Antibodies

Antibodies against p53 (DO-1) and MYCN (rabbit polyclonal, C-19) were purchased from Santa Cruz Biotechnology. Antibodies against p53Ser15-P (rabbit

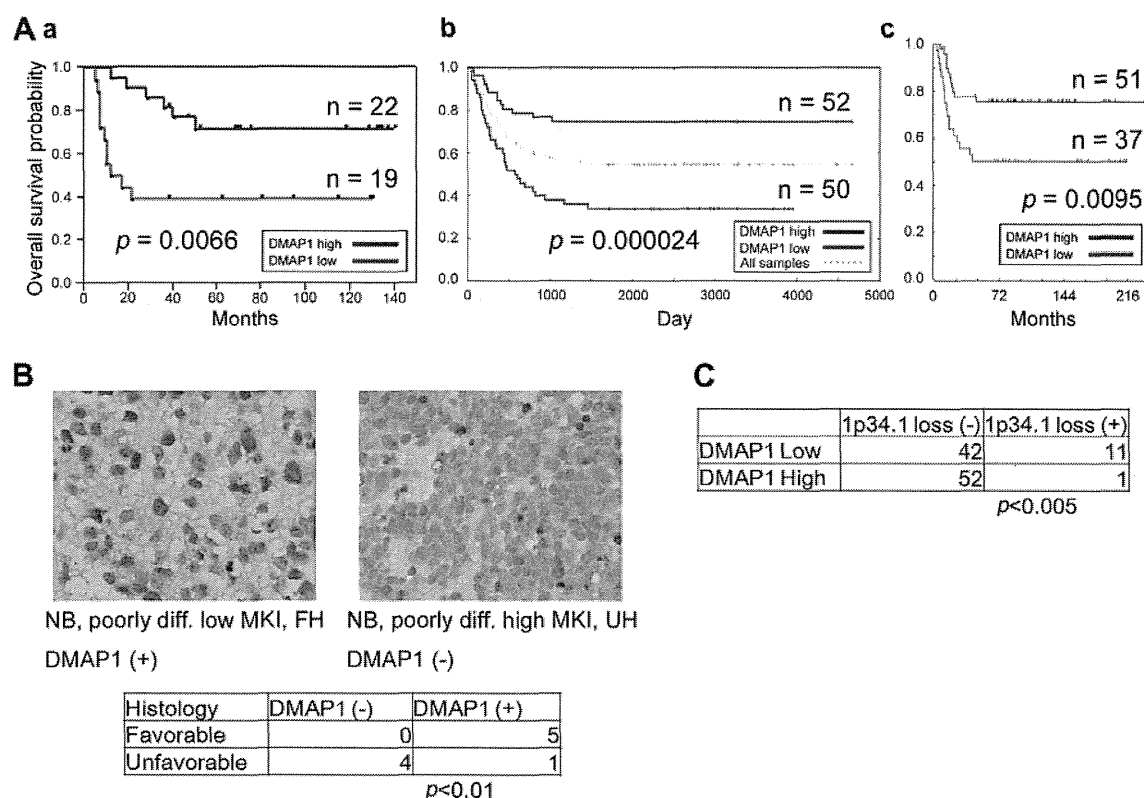


Fig. 1. Expression level of Dnmt1-associated protein 1 (DMAP1) in neuroblastoma (NB) samples and neuroblastoma cell lines. (A) Kaplan–Meier survival analysis of NB patients based on higher or lower expression levels of *DAMP1* (overall survival analysis) presented by microarray analysis in three individual cohorts. (Aa) Chiba Cancer Center Research Institute cohort ($n = 41$). Expression levels of *DAMP1* were separated into a high or low group based on the average expression. Statistical analysis was performed by the log-rank test. Corresponding p values are indicated. (Ab) Childrens Hospital Los Angeles cohort (<http://pub.abcc.ncifcrf.gov/cgi-bin/JK>), Neuroblastoma Prognosis Database–Seeger Lab dataset. $n = 102$. Expression levels of *DAMP1* on probe 224163_s_at were separated into a high or low group based on the median expression. (Ac) Academic Medical Center cohort R2 microarray analysis and visualisation platform (<http://r2.amc.nl>), Tumor Neuroblastoma public–Versteeg–88 dataset. $n = 88$. Expression levels of *DAMP1* on probe 224163_s_at were separated into a high or low group based on the expression cutoff value 118.0 according to the R2 algorithm. (B) Immunohistochemical staining for DMAP1 in NB. Statistical significance was determined by Fisher’s exact probability test. MKI: Mitosis–karyorrhexis index. FH: favourable histology; UH: unfavourable histology. DMAP1 (+): DMAP1 high-expression tumour; DMAP1 (–): DMAP1 low-expression tumour. (C) 1p loss was studied by array CGH analysis. Expression status of *DAMP1* was quantified by quantitative polymerase chain reaction (qPCR) analysis and normalised by *GAPDH* expression. *DAMP1* high or low expression was determined by its median value. Fisher’s exact probability test was applied to determine statistical significance.

polyclonal) and ATMSer1981-P (10H11. E12) were from Cell Signaling Technology (Danvers, MA, USA). Anti-ATM rabbit polyclonal antibody (Ab-3) was from Merck Millipore. Antibodies against β -Actin (rabbit polyclonal) and anti-FLAG (M2) were from Sigma–Aldrich. A mouse monoclonal anti-tubulin antibody was from Neomarkers Lab Vision (Fremont, CA, USA). Anti-DMAP1 rabbit polyclonal antibody (ab2848) was from Abcam (Cambridge, United Kingdom (UK)), anti-DMAP1 (2G12) was from Abnova (Taipei, Taiwan) and anti-human influenza hemagglutinin (HA) rabbit polyclonal was from MBL (Nagoya, Japan).

2.4. Statistical analysis

All data were tested statistically using the Welch test and Fisher’s exact probability test. $p < 0.05$ was considered to indicate statistical significance. Kaplan–Meier survival curves were calculated, and survival distributions

were compared using the log-rank test. Cox regression models were used to explore associations between *DMAP1* expression, age at diagnosis, tumour stage, *TrkA* expression, *MYCN* copy number, tumour origin, DNA ploidy, Shimada pathology and survival. Statistical significance was declared if $p < 0.05$. Statistical analysis was performed using JMP 8.0 (SAS Institute Inc., Cary, NC, USA).

Other methods are described in Supplementary information.

3. Results

3.1. Low expression level of *DMAP1* correlated with unfavourable prognosis of NB patients

We examined the expression levels of *DMAP1* in NB samples by microarray analysis. Kaplan–Meier survival analysis showed that low *DMAP1* expression correlated

with the unfavourable prognosis of NB patients (Fig. 1Aa). Web-based microarray analysis and visualisation application for NB confirmed these results (Fig. 1Ab, c), and it was also shown by quantitative polymerase chain reaction (qPCR) (Suppl. Fig. S1Aa). Unfavourable NBs, which are classified by International Neuroblastoma Staging System (INSS) stage with *MYCN* copy number, also expressed low-level *DMAPI* (Suppl. Fig. S1B). Immunohistochemical analysis also showed low expression of *DMAPI* in unfavourable histology NB (Fig. 1B).

Next, the chromosome 1p status was analysed by array CGH to study the mechanism of *DMAPI* reduction in unfavourable NB (Fig. 1C). As a result, *DMAPI* reduction in unfavourable NB was significantly correlated with loss of its gene locus. *DMAPI* mRNA levels were significantly lower in NB cell lines than in primary NB samples (Suppl. Fig. S1C). To further assess other possibilities for the suppression of *DMAPI* expression, bisulphite sequencing was carried out using five clinical samples and two cell lines of NB and *BMII* knockdown to study epigenetic suppression by polycombs in NB cell lines; however, DNA methylation of the *DMAPI* promoter region and transcriptional suppression of *DMAPI* by *BMII* were not found (data not shown). Next, univariate Cox regression was employed to examine the individual relationship of each variable to survival (Table 1). These variables were: *DMAPI* expression, age at diagnosis (>1 year old versus <1 year old), tumour stage (3 + 4 versus 1 + 2 + 4s), *TrkA* expression (low versus high), *MYCN* copy number (amplified versus non-amplified), origin (adrenal gland versus others), DNA ploidy (aneuploidy versus di-/tetraploidy) and Shimada pathology (favourable versus unfavourable), all of which were found statistically to be of prognostic importance. Additionally, multivariable Cox analysis demonstrated that *DMAPI* expression was an independent prognostic factor from tumour origin, stage and DNA ploidy. However, the analysis showed a correlation between *DMAPI* reduction and *MYCN* amplification (Table 1). These results suggested that *DMAPI* works as a tumour suppressor gene in NB and its expression levels strongly correlate with *MYCN* copy numbers.

3.2. *DMAPI* activated ATM and p53 with DNA damage

In our previous study, we observed that *Dmap1* knockdown in MEFs leads to the failure of DNA repair, resulting in accumulated DNA damage [11]. These results prompted us to study the role of *DMAPI* in DDR, including the ATM/p53 pathway. In response to DNA damage, ATM forms foci at double-stranded DNA break (DSB) sites and undergoes self-phosphorylation at serine 1981 to enhance its kinase activity. The activated ATM phosphorylates p53 at serine 15, which in turn induces p53-downstream effectors, leading to

Table 1

Correlation between *Dnmt1*-associated protein 1 (*DMAPI*) expression and other prognostic factors of neuroblastoma.

Terms	High <i>DMAPI</i>	Low <i>DMAPI</i>	<i>p</i> -Value
Age (years)			
≤1.5	25	33	0.13
>1.5	31	23	
Tumour origin			
Adrenal	29	28	0.773
Others	26	28	
Stage			
1, 2, 4S	29	22	0.184
3, 4	27	34	
Shimada pathology			
Favourable	37	30	0.16
Unfavourable	12	18	
<i>MYCN</i> copy number			
Single	52	41	<0.01
Amplified	4	15	
<i>TrkA</i> expression			
High	32	28	0.507
Low	23	26	
DNA index			
Diploidy	22	27	0.186
Aneuploidy	28	20	

MYCN: Fisher's exact probability test, $\chi^2 = 7.669496321$, $p < 0.01$.

the inhibition of cell cycle progression or apoptotic cell death [14]. For DNA damage induction, we chose doxorubicin (Doxo) at 0.5 $\mu\text{g/ml}$ concentration to assess the effect on NB cells according to the results of the analysis of peak plasma concentrations of doxorubicin [15].

We expressed *DMAPI* in p53-wild type NB cells and found that ATM Ser1981 phosphorylation increased for up to 6 h after Doxo treatment, and p53 Ser15 phosphorylation was up-regulated subsequently (Fig. 2A). We also confirmed *DMAPI*-related p53 Ser15 phosphorylation in human fibroblasts (Fig. 2B).

Next, SH-SY5Y cells, which express rather higher *DMAPI* than other NB cell lines (Suppl. Fig. S1D), were infected with sh*DMAPI*-expressing virus and treated with Doxo. Knockdown of *DMAPI* resulted in downregulation of ATM and p53 phosphorylation (Fig. 2C). We then evaluated the focus formation of ATM. It was significantly suppressed 1.0 h but not 1.5–2.5 h after Doxo treatment by *DMAPI* knockdown (Fig. 2D), suggesting that *DMAPI* is required for efficient focus formation of ATM in the early stage of DDR.

3.3. *DMAPI* activated p53 by ATM and induced transcription of p53-downstream genes

To examine whether p53 phosphorylation promoted by *DMAPI* is dependent on ATM activity, we used an

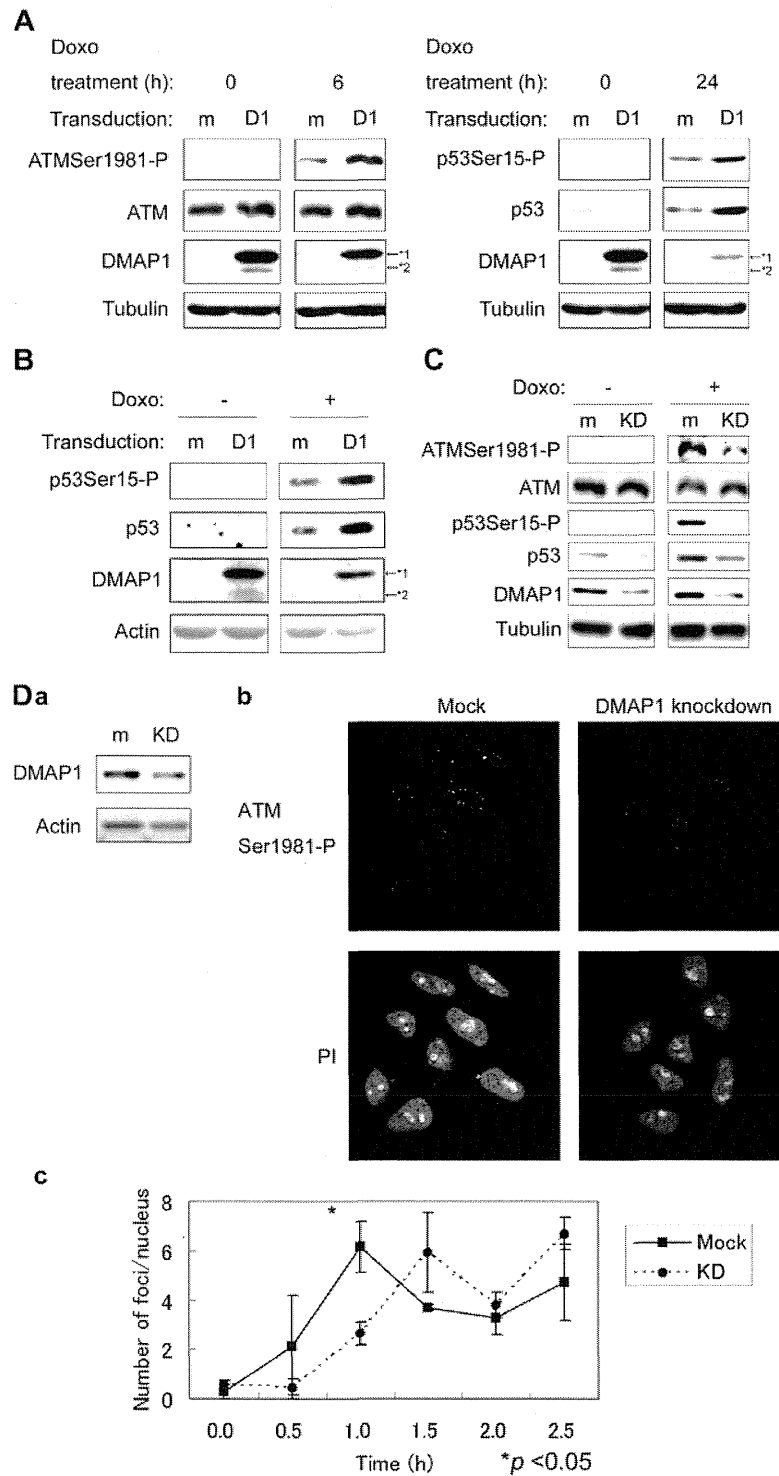


Fig. 2. Dnmt1-associated protein 1 (DMAP1) promoted focus formation of ataxia telangiectasia mutated (ATM) and activated ATM under doxorubicin (Doxo) treatment. (A) Phosphorylation status of ATMSer1981 and p53Ser15 in DMAP1 over-expressing cells. SK-N-SH cells were transduced with human influenza hemagglutinin (HA)-tagged DMAP1 and treated with Doxo for the indicated time period. The cells were subjected to sodium dodecyl sulphate-polyacrylamide gel electrophoresis (SDS-PAGE) and Western blot analysis. (B) Phosphorylation of p53Ser15 by DMAP1 in human fibroblasts (hfb). Hfb were transduced with HA-tagged DMAP1 and treated with Doxo for 24 h to confirm phosphorylation of p53 by Western blot analysis. (C) Phosphorylation status of ATMSer1981 in DMAP1 knocked-down cells. SH-SY5Y cells were infected with shDMAP1-expressing virus and treated with Doxo for 1 h. The cells were subjected to SDS-PAGE and Western blot analysis. (D) Focus formation of ATM in DMAP1 knocked-down cells. SH-SY5Y cells were infected with shDMAP1-expressing virus and treated with Doxo for the indicated time period, followed by SDS-PAGE, Western blot analysis (Da) and immunocytochemistry (ICC, Db). In ICC, cells were stained with anti-ATMSer1981-P and propidium iodide (PI). (Dc) Number of ATM foci was counted using the colony counting tool in Image Quant TL. Error bars represent S.D. obtained from triplicate samples. Data were analysed using the Welch test. Data are representative of three independent experiments. (A–D), m: mock, D1: DMAP1, KD: DMAP1 knockdown; *1: HA-DMAP1, *2: Endogenous DMAP1.

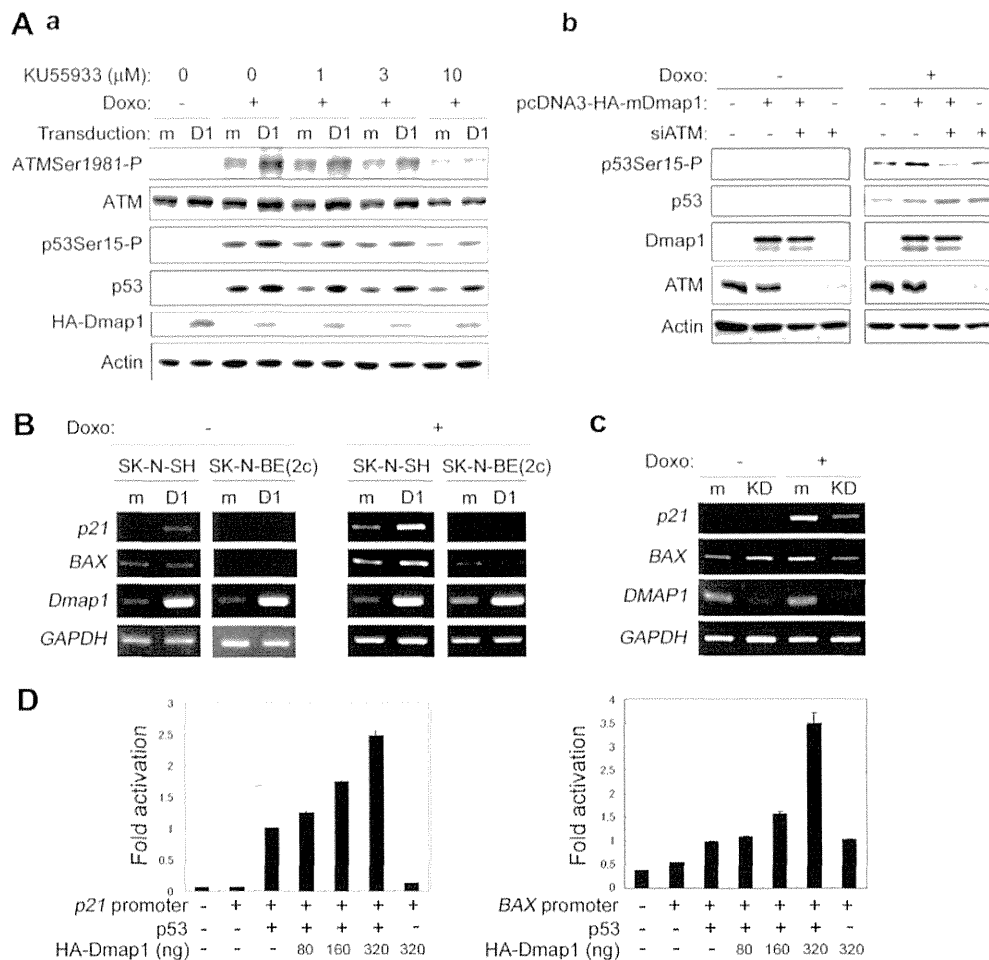


Fig. 3. Dnmt1-associated protein 1 (DMAP1) activated p53 via ataxia telangiectasia mutated (ATM). (A) Phosphorylation of p53Ser15 by Dmap1 through ATM activation. (Aa) SK-N-SH cells were infected with HA-tagged Dmap1-expressing virus and pre-treated with KU-55933. One hour after KU-55933 addition, cells were treated with doxorubicin (Doxo) for 12 h and subjected to sodium dodecyl sulphate–polyacrylamide gel electrophoresis (SDS–PAGE) and Western blot analysis. (Ab) SK-N-SH cells were transfected with *ATM* siRNA (sequence: 5'-AACATACTACTCAAAGACATT-3', Sigma–Aldrich, St. Louis, MO, USA) or control siRNA (ON-TARGETplus Non-targeting siRNA #1, Thermo Fisher Scientific, Lafayette, CO, USA). Transfection of siRNA was performed according to a previous report [16]. Forty-eight hours after forward transfection, the cells were treated with 0.3 μg/ml Doxo for 1 h and subjected to Western blot. m: mock, D1: Dmap1. (B, C) Semi-quantitative Reverse Transcription Polymerase Chain Reaction (RT-PCR) of p53-target genes in *Dmap1* over-expressing cells (B) and in DMAP1 knocked-down SH-SY5Y cells (C). m: mock, D1: Dmap1, KD: DMAP1 knockdown. (D) Luciferase reporter assay analysis of *p21^{Cip1/Waf1}* and *BAX* promoter activity in H1299 cells. Increasing amount of pcDNA3-HA-Dmap1, constant amount of pcDNA 3-p53, Renilla luciferase reporter plasmid (pRL-TK) and luciferase reporter plasmid with p53 responsive elements were transfected, and luciferase activity was studied. Data are representative of three independent experiments ($n = 3$).

ATM-specific ATP-competitive inhibitor KU-55933. KU-55933 abrogated the Dmap1-induced phosphorylation of ATM and p53, indicating ATM dependency of Dmap1-related p53 phosphorylation (Fig. 3Aa). ATM knockdown further represented ATM-dependent p53Ser15 phosphorylation by DMAP1 (Fig. 3Ab). Downstream target genes of p53, such as *p21^{Cip1/Waf1}* and *BAX*, were induced by Dmap1 in the presence or absence of Doxo in p53-wt SK-N-SH cells but were not induced in p53-mutated SK-N-BE(2c) cells (Fig. 3B). Knockdown of DMAP1 reduced p53 accumulation (Fig. 2C) and transcription of the downstream *p21^{Cip1/Waf1}* and *BAX* in a Doxo-dependent manner (Fig. 3C). Transcription of *NOXA*, the pro-apoptotic

Bcl-2 family molecule, which was previously shown to be a critical molecule in p53-related damage-induced NB cell death [16], was also upregulated by DMAP1 (Suppl. Fig. S2A). DMAP1-promoted upregulation of *p21^{Cip1/Waf1}* and *BAX* promoter activity, which was mediated by p53, was confirmed by a luciferase reporter assay of p53-null H1299 cells (Fig. 3D).

3.4. DMAP1 acts as a tumour suppressor via p53 activation in NB cells

We examined the functional role of DMAP1 and its p53 dependency in NB cells. DMAP1 enhanced cell cycle arrest and apoptosis induced by Doxo in a

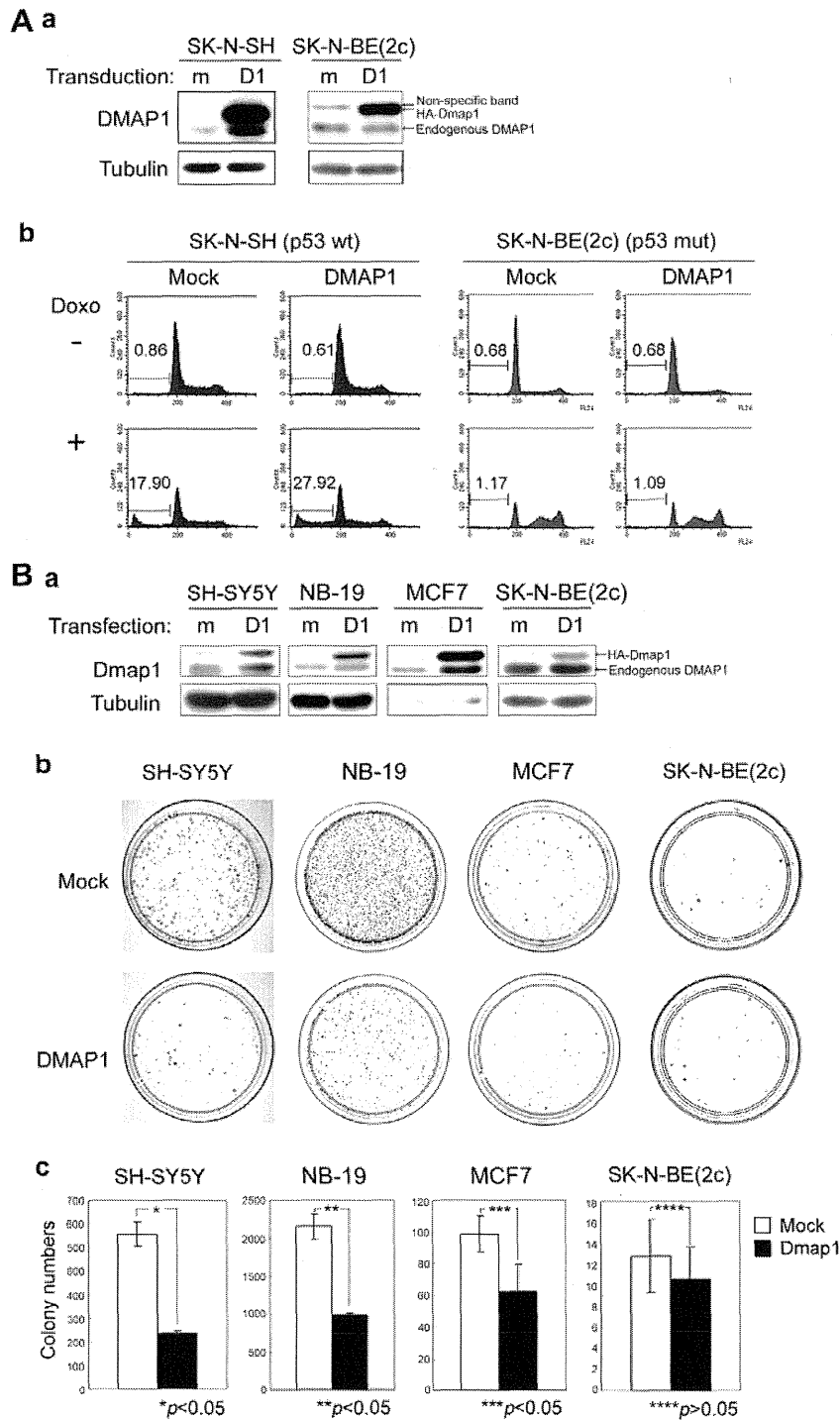


Fig. 4. Dnmt1-associated protein 1 (DMAP1) acts as a tumour suppressor via p53 activation in NB cells. (A) Dmap1-transduced NB cells were treated with doxorubicin (Doxo) and subjected to Western blot (Aa) and cell cycle analysis by flow cytometry (Ab). Numbers in histogram indicate % of subG0/G1 population. (B) Colony formation assay in Dmap1 over-expressing cells. Cells were transfected with pcDNA3-heteroduplex analysis (HA)-Dmap1 and subjected to Western blot (Ba) and selected with 400 $\mu\text{g/ml}$ G418 for SH-SY5Y cells, 500 $\mu\text{g/ml}$ G418 for NB-19 cells, 800 $\mu\text{g/ml}$ G418 for MCF7 cells and 800 $\mu\text{g/ml}$ G418 for SK-N-BE(2c) cells, for 2 weeks. (Bb) Colonies were stained with May-Grünwald's Eosin Methylene Blue Solution (Wako, Osaka, Japan) and Giemsa's solution (Merk Japan, Tokyo, Japan). (Bc) Number of colonies was counted using the colony counting tool in Image Quant TL. Error bars represent S.D. (A–B), m: mock, D1: Dmap1.

p53-dependent manner (Fig. 4A and Suppl. Fig. S2B). SH-SY5Y cells, NB-19 cells and breast cancer-derived MCF7 cells harbouring wild-type p53 were transfected with pcDNA3-HA-Dmap1 and selected with G418 for

two weeks. As shown in Fig. 4B, Dmap1 significantly suppressed colony formation in these cells. These results suggested that DMAP1 acts as a tumour suppressor via p53 activation in NB cells.

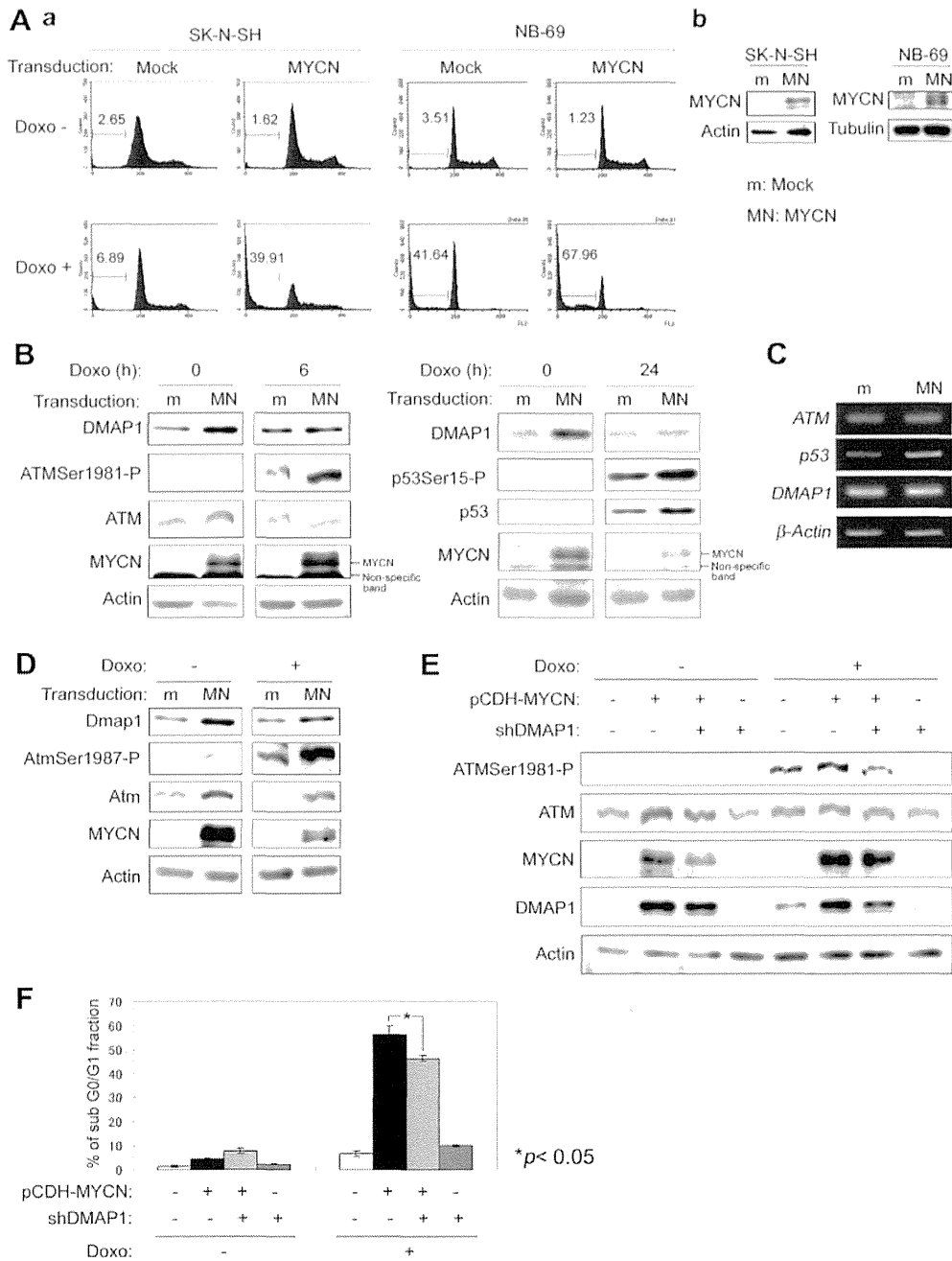


Fig. 5. MYCN promoted doxorubicin (Doxo)-induced apoptosis and ataxia telangiectasia mutated (ATM)/p53 activation. Cells were transduced with pCDH-MYCN and subjected to analysis as follows. (Aa) Cell cycle analysis [(Ab) protein expression was confirmed by Western blotting in left panel], (B) Western blot analysis and (C) semi-quantitative RT-PCR of MYCN over-expressing and Doxo-treated NB cells. Numbers in histogram indicate % of sub G0/G1 population. (D) Activation of Atm/p53 pathway by MYCN in NIH3T3 cells. Cells were collected 12 h after Doxo treatment and subjected to Western blot analysis. (E, F) MYCN over-expression and/or Dnm1-associated protein 1 (DMAP1) knockdown were performed as indicated in SK-N-SH cells. Cells were collected for Western blot analysis of ATMSer1981-P (E) and sub G0/G1 analysis (F) 6 h after Doxo treatment. (A–D) m: mock, MN: MYCN.

3.5. DMAP1 was implicated in MYCN-induced ATM activation

Given that MYCN amplification correlated with a low level of DMAP1 and that MYCN regulates the ATM/p53 pathway [17], we studied the DMAP1/ATM/p53 pathway in MYCN-transduced cells. As

reported [18], exogenous MYCN promoted apoptosis in MYCN single-copy and p53 wild type SK-N-SH cells and NB-69 cells (Fig. 5A) and activation of ATM/p53 under Doxo treatment in SK-N-SH cells (Fig. 5B left: 6 h after, right: 24 h after). Interestingly, the protein amount of DMAP1 was upregulated by MYCN although DMAP1 mRNA was not increased (Fig. 5B, C).

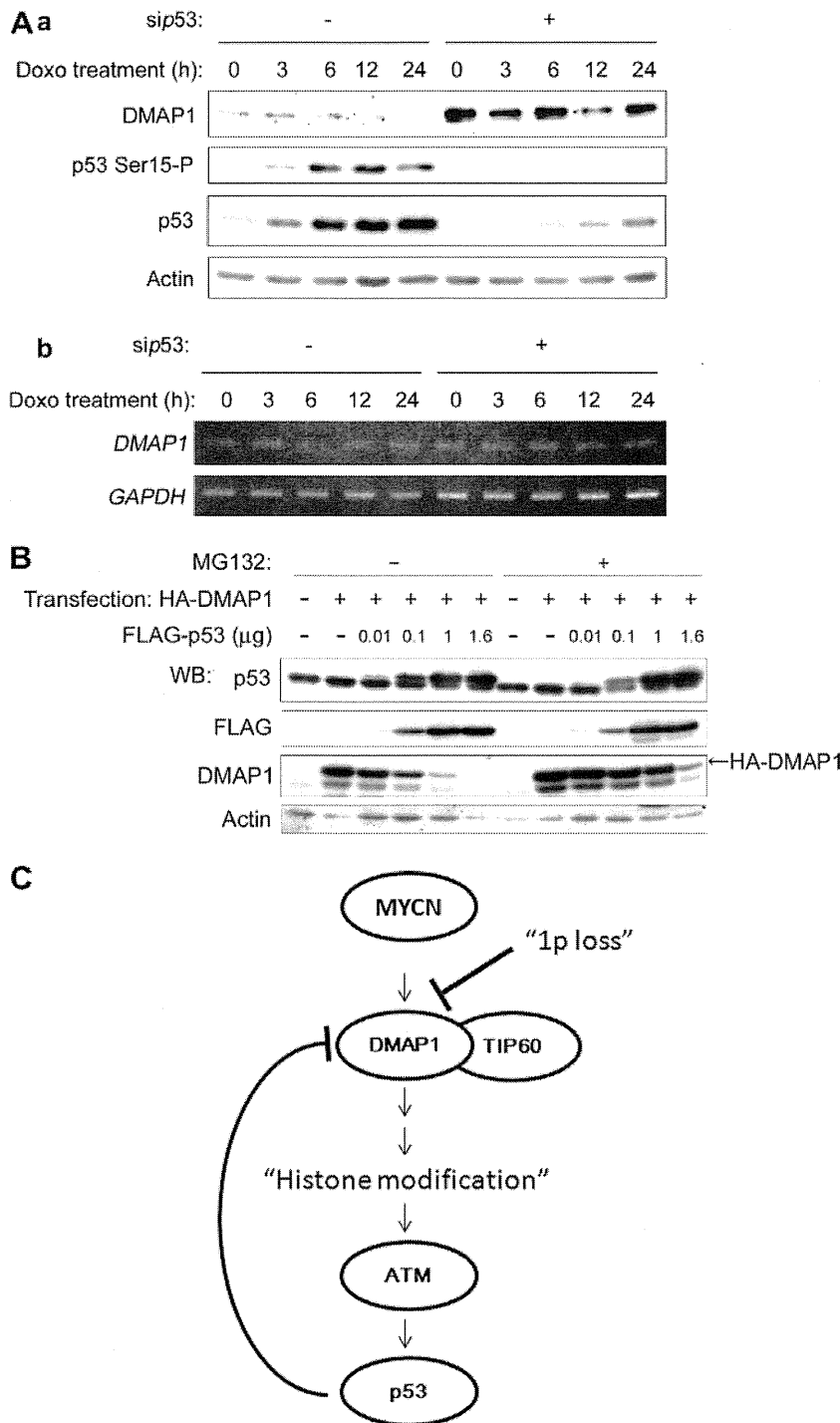


Fig. 6. Dnmt1-associated protein 1 (DMAP1) degradation by p53. (A) DMAP1 expression in p53 knocked-down cells. SK-N-SH cells harbouring wt-p53 were transfected with *p53* siRNA (ON-TARGETplus Duplex J-003329-14-0005, Human Tp53; Thermo Fisher Scientific, Lafayette, CO, USA) or control siRNA (Silencer_Negative Control #1 siRNA; Ambion Inc., Austin, TX, USA). Transfection of siRNA was performed according to a previous report (16). Forty-eight hours after forward transfection, the cells were treated with 0.3 μ g/ml doxorubicin (Doxo) for the indicated time periods and subjected to Western blotting (Aa)/semi-quantitative RT-PCR (Ab). (B) Western blot analysis of Dmap1 degradation by p53 in combination with MG132 treatment. 293T cells were transfected with a constant amount of pcDNA3-heteroduplex analysis (HA)-tagged Dmap1 and increasing amounts of pcDNA3-FLAG-tagged p53 and then treated with 2 μ M MG132 for 24 h. (C) MYCN/DMAP1/ataxia telangiectasia mutated (ATM)/p53 pathway regulates neuroblastoma cell death.

These phenomena were confirmed in *MYCN*-single copy, p53 wild-type NIH3T3 fibroblasts (Fig. 5D).

Further, DMAP1 knockdown reduced the phosphorylation of ATM (Fig. 5E) and Doxo-induced apoptosis

(Fig. 5F), which were up-regulated by MYCN, indicating that DMAP1 was implicated in MYCN-induced ATM/p53 activation and apoptosis.

3.6. Negative feedback regulation of DMAP1 by p53

In MYCN-related ATM/p53 pathway activation, we found that DMAP1 protein was reduced, accompanied with p53 activation (Fig. 5B) and this DMAP1 reduction was also observed in DMAP1-transduced cells after p53 activation by Doxo (Figs. 2A, B and 3A). To examine whether p53 reduces DMAP1, we knocked down p53 in NB cells (Fig. 6A). DMAP1 protein was clearly increased by p53 knockdown, but the mRNA level of DMAP1 was not affected. Proteasome inhibitor, MG132 treatment effectively inhibited DMAP1 degradation by p53 expression (Fig. 6B), suggesting that p53 promotes DMAP1 degradation in an ubiquitin-proteasome system-dependent manner.

4. Discussion

The proto-oncogenes *MYC* and *MYCN* have a pivotal function in growth control, differentiation and apoptosis and are among the most frequently affected genes in human malignant tumours; they are overexpressed in a large percentage of human tumours [19,20]. Transformation by Myc proteins requires concomitant inhibition of apoptosis by inactivation of apoptosis-inducing pathway genes [21]. One of the *MYC* oncogene product-related apoptotic pathways is involved in DDR [18]. Recent studies have clarified the relevant pathways regulating MYC-induced DDR, leading to the identification of ATM, TIP60 and WIP1 as mediators of this response [22]. Once ATM was activated by DNA damage, both p53 and proteins that interact with p53, MDM2 and Chk2 were phosphorylated by ATM, which in turn transactivated the p53-downstream effectors, leading to the inhibition of cell cycle progression or apoptotic cell death [23].

Regarding MYC/MYCN-related ATM regulation, this over-expression causes DNA damage *in vivo* and the ATM-dependent response to this damage is critical for p53 activation, apoptosis and the suppression of tumour development [22,24,25]. These findings suggested that MYC/MYCN expression induces ATM/p53 pathway activation by the related cellular stresses and subsequent inactivation of ATM will produce advantages for the tumorigenesis of MYC/MYCN-deregulated tumours. However, the occurrence of NB in ataxia-telangiectasia patients and ATM mutation in NB cells have not been reported to our knowledge, and mutations of p53 have been reported in <2% of NB [26,27], suggesting that functional inactivation of the pathway by other molecules seems to occur in NB tumours.

In the present study, we found that MYCN expression in *MYCN* single-copy cells increased DMAP1 and Doxo-induced apoptotic cell death (Fig. 5). DMAP1 induced ATMSer1981 phosphorylation and its focus formation in the presence of Doxo (Figs. 2 and 3A). By DMAP1 expression, p53Ser15 phosphorylation was induced in an ATM-dependent manner. In NB tumour samples, low expression of DMAP1 was related to poor prognosis, unfavourable histology, *MYCN* amplification and 1p LOH (Fig. 1, Table 1, Suppl. Fig. S1), suggesting that DMAP1 downregulation is required for NB tumorigenesis, especially under MYCN-induced cellular stress. Intriguingly, we observed negative feedback for degrading DMAP1, suggesting another DMAP1 downregulation mechanism in NB tumorigenesis (Fig. 6).

Recently, Penicud and Behrens reported that DMAP1 enhances Histone Acetyl Transferase (HAT) activity of TIP60 and promotes ATM auto-phosphorylation [12]. Depleting DMAP1 reduced ATM phosphorylation a few minutes after irradiation, but at later time points, it had no effect on ATM activation, as we previously reported [11]. Consistent with these observations, we found that DMAP1 knockdown delayed ATM focus formation and that the delay of ATM activation attenuated p53 phosphorylation and stabilisation. (Fig. 2C, D). These results indicate that DMAP1 regulates the efficient recruitment of ATM to the site of DNA breaks and this regulation is required for subsequent Doxo-induced p53-dependent cell death in NBs.

Taken together, we found that DMAP1 is a novel molecule of 1p tumour suppressors and has a role in ATM/p53 activation induced by MYCN-related cellular stresses (Fig. 6C). DMAP1 might be a new molecular target of MYCN-amplified NB treatment.

Conflict of interest statement

None declared.

Acknowledgements

We would like to thank Ms. Kumiko Sakurai and Dr. Masamitsu Negishi for technical help, and Daniel Mrozek, Medical English Service, for editorial assistance. *Grant Support:* This work was supported in part by a grant-in-aid from the National Cancer Center Research and Development Fund (4), a grant-in-aid from the Ministry of Health, Labor, and Welfare for Third Term Comprehensive Control Research for Cancer, and a Grant-in-Aid for Scientific Research (B) (24390269).

Appendix A. Supplementary data

Supplementary data associated with this article can be found, in the online version, at <http://dx.doi.org/10.1016/j.ejca.2014.01.023>.

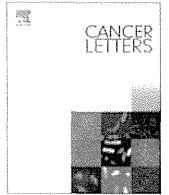
References

- [1] Brodeur GM. Neuroblastoma: biological insights into a clinical enigma. *Nat Rev Cancer* 2003;3:203–16.
- [2] Praml C, Finke LH, Herfarth C, Schlag P, Schwab M, Amler L. Deletion mapping defines different regions in 1p34.2-pter that may harbor genetic information related to human colorectal cancer. *Oncogene* 1995;11:1357–62.
- [3] Nagai H, Negrini M, Carter SL, et al. Detection and cloning of a common region of loss of heterozygosity at chromosome 1p in breast cancer. *Cancer Res* 1995;55:1752–7.
- [4] Smith JS, Perry A, Borell TJ, et al. Alterations of chromosome arms 1p and 19q as predictors of survival in oligodendrogliomas, astrocytomas, and mixed oligoastrocytomas. *J Clin Oncol* 2000;18:636–45.
- [5] Yang J, Du X, Lazar AJ, et al. Genetic aberrations of gastrointestinal stromal tumors. *Cancer* 2008;113:1532–43.
- [6] Maris JM, Weiss MJ, Guo C, et al. Loss of heterozygosity at 1p36 independently predicts for disease progression but not decreased overall survival probability in neuroblastoma patients: a Children's Cancer Group study. *J Clin Oncol* 2000;18:1888–99.
- [7] Martinsson T, Sjöberg RM, Hedborg F, Kogner P. Deletion of chromosome 1p loci and microsatellite instability in neuroblastomas analyzed with short-tandem repeat polymorphisms. *Cancer Res* 1995;55:5681–6.
- [8] White PS, Thompson PM, Gotoh T, et al. Definition and characterization of a region of 1p36.3 consistently deleted in neuroblastoma. *Oncogene* 2005;24:2684–94.
- [9] Hogarty MD, Winter CL, Liu X, et al. No evidence for the presence of an imprinted neuroblastoma suppressor gene within chromosome sub-band 1p36.3. *Cancer Res* 2002;62:6481–4.
- [10] Rountree MR, Bachman KE, Baylin SB. DNMT1 binds HDAC2 and a new co-repressor, DMAP1, to form a complex at replication foci. *Nat Genet* 2000;25:269–77.
- [11] Negishi M, Chiba T, Saraya A, Miyagi S, Iwama A. Dmap1 plays an essential role in the maintenance of genome integrity through the DNA repair process. *Genes Cells* 2009;14:1347–57.
- [12] Penicud K, Behrens A. DMAP1 is an essential regulator of ATM activity and function. *Oncogene* 2014;33:525–31.
- [13] Takenobu H, Shimozato O, Nakamura T, et al. CD133 suppresses neuroblastoma cell differentiation via signal pathway modification. *Oncogene* 2011;30:97–105.
- [14] Lavin MF. Ataxia-telangiectasia: from a rare disorder to a paradigm for cell signalling and cancer. *Nat Rev Mol Cell Biol* 2008;9:759–69.
- [15] James HD. Topoisomerase II inhibitors: anthracyclines. In: Chabner BA, Longo DL, editors. *Cancer chemotherapy and biotherapy: principles and practice*. Philadelphia: Lippincott Williams & Wilkins, a Wolters Kluwer Business; 2011. p. 356–91.
- [16] Shi Y, Takenobu H, Kurata K, et al. HDM2 impairs Noxa transcription and affects apoptotic cell death in a p53/p73-dependent manner in neuroblastoma. *Eur J Cancer* 2010;46:2324–34.
- [17] Hu H, Du L, Nagabayashi G, Seeger RC, Gatti RA. ATM is down-regulated by N-Myc-regulated microRNA-421. *Proc Natl Acad Sci U S A* 2010;107:1506–11.
- [18] Fulda S, Lutz W, Schwab M, Debatin KM. MycN sensitizes neuroblastoma cells for drug-induced apoptosis. *Oncogene* 1999;18:1479–86.
- [19] Evan GI, Littlewood TD. The role of c-myc in cell growth. *Curr Opin Genet Dev* 1993;3:44–9.
- [20] Schwab M, Alitalo K, Klempnauer KH, et al. Amplified DNA with limited homology to myc cellular oncogene is shared by human neuroblastoma cell lines and a neuroblastoma tumour. *Nature* 1983;305:245–8.
- [21] Gustafson WC, Weiss WA. Myc proteins as therapeutic targets. *Oncogene* 2010;29:1249–59.
- [22] Campaner S, Amati B. Two sides of the Myc-induced DNA damage response: from tumor suppression to tumor maintenance. *Cell Div* 2012;7:6.
- [23] Derheimer FA, Kastan MB. Multiple roles of ATM in monitoring and maintaining DNA integrity. *FEBS Lett* 2010;584:3675–81.
- [24] Petroni M, Veschi V, Prodosmo A, et al. MYCN sensitizes human neuroblastoma to apoptosis by HIPK2 activation through a DNA damage response. *Mol Cancer Res* 2011;9:67–77.
- [25] Swift M, Reitnauer PJ, Morrell D, Chase CL. Breast and other cancers in families with ataxia-telangiectasia. *N Engl J Med* 1987;316:1289–94.
- [26] Vogan K, Bernstein M, Leclerc JM, Brisson L, Brossard J, Brodeur GM, et al. Absence of p53 gene mutations in primary neuroblastomas. *Cancer Res* 1993;53:5269–73.
- [27] Tweddle DA, Malcolm AJ, Bown N, Pearson AD, Lunec J. Evidence for the development of p53 mutations after cytotoxic therapy in a neuroblastoma cell line. *Cancer Res* 2001;61:8–13. <http://cancerres.aacrjournals.org/content/61/1/8.long>.



Contents lists available at ScienceDirect

Cancer Letters

journal homepage: www.elsevier.com/locate/canlet

RASSF1A methylation may have two biological roles in neuroblastoma tumorigenesis depending on the ploidy status and age of patients [☆]

Masayuki Haruta ^a, Takehiko Kamijo ^b, Akira Nakagawara ^b, Yasuhiko Kaneko ^{a,*}

^a Research Institute for Clinical Oncology, Saitama Cancer Center, Ina, Saitama, Japan

^b Research Institute, Chiba Cancer Center, Chiba, Japan

ARTICLE INFO

Article history:

Received 3 September 2013

Received in revised form 19 March 2014

Accepted 19 March 2014

Available online xxxx

Keywords:

Neuroblastoma

Mass-screening

RASSF1A methylation

Triploid

Diploid

ABSTRACT

RASSF1A methylation was frequent in neuroblastomas found in infants by mass-screening or infants and children diagnosed clinically, whereas *CASP8* and *DCR2* methylation was only frequent in tumors in children. When classified according to the ploidy status, RASSF1A and *PCDHB* methylation was only associated with *MYCN* amplification and poor outcomes in infants with a clinically diagnosed diploid, not triploid tumor. RASSF1A and *PCDHB* methylation was associated with poor outcomes in children with triploid and diploid tumors, respectively, and with *MYCN* amplification in children with diploid tumor. RASSF1A methylation may have two biological roles based on the ploidy status and patient's age.

© 2014 Elsevier Ireland Ltd. All rights reserved.

1. Introduction

Neuroblastoma is the most common solid tumor in children, and accounts for 8–10% of childhood cancers and 15% of childhood cancer deaths [1]. While localized neuroblastomas in infants regress spontaneously or mature, disseminated tumors in children resist intensive multimodal treatment [2,3]. A mass-screening program has been conducted on infants in Japan and other countries, based on the assumption that the early detection of tumors in infants could improve overall outcomes [4–6]. Because it is clear that damage has been caused by excessive treatment of some neuroblastomas that would have regressed spontaneously, and the effectiveness of the program has been questioned [5–7], this program was discontinued in Japan.

RASSF1A functions as a tumor suppressor gene that plays an important role in cell cycle arrest, apoptosis, genomic stability, microtubule stabilization, and cell motility [8–10]. The mRNA expression levels of RASSF1A are controlled by DNA methylation in the promoter region, and it is a representative gene that shows hypermethylation in various primary tumors [8,11–24]. Caspase 8

encoded by *CASP8* is a family member of cysteine proteases that play essential roles in apoptosis, and silencing of *CASP8* by methylation has frequently been found in neuroblastomas, especially those with *MYCN* amplification [14–19,21,22,24–28]. *DCR2* has been shown to prevent binding of TNF-related apoptosis-inducing ligand (TRAIL) to the death receptors, DR4 and DR5 as a decoy receptor, and exhibits antiapoptotic activity. The down-regulation of *DCR2* by promoter methylation was reported in various types of cancer including neuroblastoma [29,30]. In addition, the CpG island methylator phenotype (CIMP) was shown to have stronger prognostic power than methylation of individual genes in neuroblastomas; CIMP was detected by methylation analysis of the *PCDHB* CGIs [31].

Tumor cell ploidy is one of the biomarkers that predicts outcomes of patients with neuroblastoma. The majority of tumors found by mass-screening have been characterized by triploidy [32]. The International Neuroblastoma Risk Group (INRG) classification system used ploidy (DNA index) to classify tumors with distant metastasis and less than 18 months of age [33].

Many studies have examined the methylation status of tumor suppressor genes in neuroblastomas; however, none have clarified the association between methylation of the genes and the subtypes of tumors classified by age, method for tumor detection, or the ploidy status, although the disease is well-known for its biological heterogeneity [14–28]. We found that RASSF1A, *CASP8*, *DCR2*, and *PCDHB* family were significantly methylated, and associated with clinical and *MYCN* status. When tumors were classified according

[☆] Grant sponsors: The Ministry of Health, Welfare and Labor of Japan (for Second-Term Comprehensive 10-Year Strategy for Cancer Control).

* Corresponding author at: Division of Cancer Diagnosis, Research Institute for Clinical Oncology, Saitama Cancer Center, Ina, Saitama, Japan. Tel.: +81 48 722 1111; fax: +81 48 723 5197.

E-mail address: kaneko@cancer-c.pref.saitama.jp (Y. Kaneko).

to the ploidy status, *RASSF1A* and *DCR2* methylation was associated with poor outcomes in infants with a diploid, not triploid tumor, and in children with a triploid, not diploid tumor, suggesting age-dependent heterogeneity in triploid tumors.

2. Material and methods

2.1. Patients and samples

Tumors were obtained from 259 Japanese infants or children with neuroblastoma who underwent biopsy or surgery between January 1985 and December 1998. One-hundred and twenty-three patients were found by mass-screening to have neuroblastomas at 6 months of age (group A1) and 64 patients at 18 months of age or less (group A2), and 72 children over 18 months (group B) were diagnosed clinically.

2.2. Ploidy determined by interphase FISH and flow cytometry

Pathologists in each institution verified that each sample contained 70% or more tumor cells. To detect the copy number of chromosome 1s and the status of 1p, two-color FISH was performed using the two probes, D1Z1 and D1Z2, as described previously [34]. Disomy 1, trisomy 1, tetrasomy 1, or pentasomy 1 was determined based on the number of D1Z1 signals. The DNA index of tumor tissues was analyzed on the Becton–Dickinson FACScan flow cytometer by DNA cell-cycle analysis software-version C. Tumors were classified into 2 types (diploid, 2n and triploid, 3n) based on the numbers of chromosome 1 or the DNA index obtained by flow cytometry. Triploidy included triploidy and hyperdiploidy determined by flow cytometry, and tumors with a combination of cells with 3, 4, and 5 chromosomes 1 examined by FISH were classified as triploid (3n) tumors.

2.3. Sodium bisulfite modification and conventional methylation-specific PCR (MSP) analysis

Bisulfite treatment was performed as previously described [11,35]. The genes examined were *RASSF1A*, *CASP8*, *DCR2*, *HOXA9*, *RUNX3*, *NORE1A*, *p16INK4A*, *p14ARF*, *RASSF2A*, *SOCS1*, *RIZ1*, and *HOXB5*. Primer sequences and PCR conditions were described in a previous study [11]. PCR products were run on 2% agarose gels and visualized after staining with ethidium bromide.

2.4. Quantitative MSP analyses of *RASSF1A*, *DCR2*, and *PCDHB* family

Bisulfite-modified DNA was used as a template for TaqMan- or SYBR green I-based real-time PCR using a LightCycler (Roche Diagnostics), as described previously [11]. Primers and probes used to specifically amplify bisulfite-converted DNA for the internal reference gene (*ACTB*) and target genes (*RASSF1A*, *DCR2*, and *PCDHB* family) were described in Supplementary Table 1 [11,31]. Each amplification reaction included positive and negative controls for the methylation status of target genes, and tumor DNA samples with the bisulfite treatment. *ACTB* was used as a reference gene to determine the relative level of methylated DNA for one of the target genes in each sample.

We failed to detect quantitative PCR products using PCR primers and a probe for the exon 4 region of *CASP8*, from which PCR primer sequences for conventional PCR were obtained, probably because of low CpG contents of the region.

2.5. *MYCN* amplification analysis

DNA preparation, digestion, and Southern blot analysis using the *MYCN* probe were performed as described previously [34]. More than 3 copies of the *MYCN* gene per haploid genome were considered to indicate amplification.

2.6. Statistical analysis

The significance of differences in various biological and clinical aspects of the disease among the patient groups was examined by the Chi-square or Fisher's exact test. The Student's *t* test with or without Welch's correction compared the mean percentages of *RASSF1A*, *DCR2*, or *PCDHB* methylation between two types of tumors with or without *MYCN* amplification or any two ploidy groups classified by the age of patients and the method of tumor detection. The overall survival for each group of patients was estimated on August 30, 2003 by the Kaplan–Meier method, and compared using log-rank tests. The survival time was defined as the interval between remission induction or surgery and death from any cause. The influence of various biological and clinical factors on overall survival was estimated using the Cox proportional-hazards model calculated with Stat Flex software for Windows, version 6.0.

3. Results

3.1. Conventional and quantitative MSP analysis

The methylation status of *RASSF1A*, *CASP8*, *DCR2*, *HOXA9*, *RUNX3*, *NORE1A*, *p16INK4A*, *p14ARF*, *RASSF2A*, *SOCS1*, *RIZ1*, and *HOXB5* was examined using conventional MSP. Conventional MSP analysis of the *RASSF1A*, *CASP8*, and *DCR2* genes was performed in 259 neuroblastomas [123 found by mass-screening (group A1) and 136 found clinically (groups A2 + B)], and of the other 9 genes in 45 tumors (25 found by mass-screening and 20 diagnosed clinically). *RASSF1A*, *CASP8*, and *DCR2* were methylated in 57.7%, 3.3%, and 3.3% of 123 neuroblastomas found by mass-screening, in 51.6%, 10.9%, and 1.6% of 64 tumors diagnosed clinically (<18 months), and in 70.8%, 40.3%, and 38.9% of 72 tumors diagnosed clinically (>18 months) (Supplementary Tables 2–4). None of the 9 other genes (*HOXA9*, *RUNX3*, *NORE1A*, *p16INK4A*, *p14ARF*, *RASSF2A*, *SOCS1*, *RIZ1*, and *HOXB5*) were methylated in the 45 tumors.

Quantitative MSP analysis of *RASSF1A*, *DCR2*, and *PCDHB* methylation was carried out in 221 (85.3%), 116 (44.8%), and 116 (44.8%), respectively, of 259 neuroblastomas. Group A1 was included in *RASSF1A* analysis, and excluded from *DCR2* and *PCDHB* analysis. We performed ROC analysis, and determined cut-off values of 26%, 7%, and 18% of *RASSF1A*, *DCR2*, and *PCDHB* methylation (Fig. 1, A, B, and C). We then examined the dose–response relationship between percentages of *RASSF1A*, *DCR2* and *PCDHB* methylation (10%, 20%, 30%, 40%, 50%, 60%, 70% and 80%) and overall survival, and adopted the cut-off value of 40%, 70%, and 60%, respectively, which gave the highest HR (Fig. 1D–F). Although cut-off values were determined based on data of overall survival, they were also used for association analysis between gene methylation and clinical and *MYCN* features.

3.2. Correlation between *RASSF1A*, *CASP8*, *DCR2*, and *PCDHB* methylation and stage of the disease

We found no significant difference in stage distribution between *RASSF1A*-, *CASP8*-, and *DCR2*-methylated tumors and *RASSF1A*-, *CASP8*-, and *DCR2*-unmethylated tumors, respectively, determined by conventional MSP and found by mass-screening with an exception of *RASSF1A*-methylated diploid tumors (Table 1). *RASSF1A*-methylated tumors were at more advanced stages than *RASSF1A*-unmethylated tumors in infants and children diagnosed clinically ($P = 0.018$ and $P = 5.49E-05$). Quantitative MSP analysis confirmed the association. *CASP8*- and *DCR2*-methylated tumors were at a more advanced stage than *CASP8*- and *DCR2*-unmethylated tumors in children ($P = 0.026$ and $P = 5.06E-05$), however, such an association was not detected in tumors in infants diagnosed clinically. Quantitative MSP analysis of *DCR2* confirmed the association between the methylation and an advanced stage in children, but not in infants. The similar association was also found between *PCDHB*-methylated and -unmethylated tumors in children.

When tumors were further classified according to the ploidy status, *RASSF1A*-methylated diploid tumors were or were more likely to be a more advanced stage than *RASSF1A*-unmethylated diploid tumors in infants found by mass-screening ($P = 0.029$) or clinically diagnosed (<18 months) ($P = 0.052$) and in children (>18 months) ($P = 0.006$) (Table 1). *RASSF1A*-methylated triploid tumors in children were at a more advanced stage than *RASSF1A*-unmethylated triploid tumors in children ($P = 3.12E-03$), but not in infants found by mass-screening or clinically diagnosed. Quantitative MSP could not confirm the association in children.

Children with *CASP8*-methylated tumors were at a more advanced stage than those with *CASP8* unmethylated tumors in children ($P = 0.026$). *DCR2*-methylated diploid and triploid tumors in

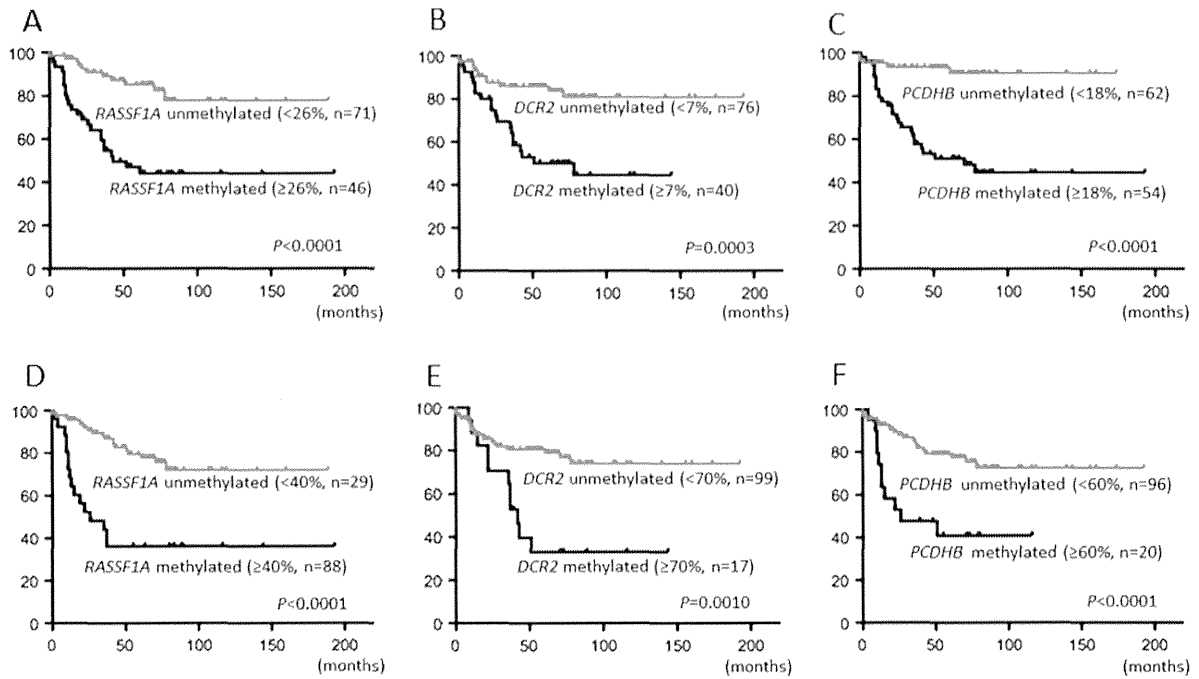


Fig. 1. Overall survival curves for infants and children diagnosed clinically and classified by the cut-off value in tumors determined by ROC analysis; (A) RASSF1A, 26% [$P < 0.0001$, hazard ratio (HR) 4.634, 95% confidence interval (95%CI) 2.3–9.3]; (B) DCR2, 7% ($P = 0.0003$, HR 3.91, 95%CI 1.9–8.2); (C) PCDHB, 18% ($P < 0.0001$, HR 5.35, 95%CI 2.7–10.8), and by the dose–response relationship; (D) RASSF1A, 40% ($P < 0.0001$, 7.89, 95%CI 3.3–19.2); (E) DCR2, 70% ($P = 0.001$, 5.34, 95%CI 2.0–14.5); (F) PCDHB, 60% ($P < 0.0001$, 6.11, 95%CI 2.2–16.9).

Table 1
Association between RASSF1A, CASP8, DCR2, and PCDHB methylation and stage of the disease.

	Group A1 (≤18 m)	Group A2 (≤18 m)	Group B (>18 m)		Group A2 (≤18 m)	Group B (>18 m)
RASSF1A (cMSP)				RASSF1A (qMSP)		
Total (methyl versus unmethyl)	NS	S (0.018)	S (5.49E–05)		ROC, S (0.029); DRR., NS	ROC, S (0.008); DRR., S (0.022)
Diploidy (methyl versus unmethyl)	S (0.029)	M (0.052)	S (0.006)		ROC, NS; DRR., NS	ROC, M (0.078); DRR., NS
Triploidy (methyl versus unmethyl)	NS	NS	S (3.12E–03)	ROC, NS; DRR, NA	ROC, M (0.080); DRR., NS	
CASP8 (cMSP)						
Total (methyl versus unmethyl)	NS	M (0.090)	S (0.026)			
Diploidy (methyl versus unmethyl)	NA	NS	NS			
Triploidy (methyl versus unmethyl)	NS	NA	NS			
DCR2 (cMSP)				DCR2 (qMSP)		
Total (methyl versus unmethyl)	NS	NS	S (5.06E–05)		ROC, NS; DRR, NA.	ROC, S (0.005); DRR., S (0.004)
Diploidy (methyl versus unmethyl)	NS	NS	S (0.003)		ROC, NS; DRR, NA	ROC, M (0.057); DRR., S (0.033)
Triploidy (methyl versus unmethyl)	NS	NA	S (0.017)	ROC, NA ; DRR, NA	ROC, S (0.048); DRR., NS	
PCDHB				PCDHB (qMSP)		
Total (methyl versus unmethyl)					ROC, NS; DRR., NS	ROC, S (5.70E–06); DRR., M (0.051)
Diploidy (methyl versus unmethyl)					ROC, NS; DRR., NS	ROC, S (0.001); DRR., NS
Triploidy (methyl versus unmethyl)				ROC, NS; DRR, NS	ROC, S (0.003); DRR., NS	

Group A1, infants found by mass-screening; Group A2, infants diagnosed clinically; Group B, children diagnosed clinically; m, month; cMSP, conventional methylation-specific PCR; qMSP, quantitative methylation-specific PCR; Methyl, methylated; unmethyl, unmethylated; NS, not significant; S, significant; M, marginally significant; NA, not applicable; ROC, ROC analysis; DRR, dose–response relationship analysis; Detailed data are shown in Supplementary Tables 2–7.